Enantioresolution of Chiral Derivatives of Xanthones on (*S,S*)-Whelk-O1 and L-Phenylglycine Stationary Phases and Chiral Recognition Mechanism by Docking Approach for (*S,S*)-Whelk-O1

CARLA FERNANDES,[1,2] ANDREIA PALMEIRA,[1,2] ALEXANDRE SANTOS,[1,2] MARIA ELIZABETH TIRITAN,[1,3] CARLOS AFONSO,[1,2] AND MADALENA M. PINTO[1,2]*

[1]*Centro de Química Medicinal da, Universidade do Porto (CEQUIMED-UP), Rua de Jorge Viterbo Ferreira 228, 4050-313, Porto, Portugal*
[2]*Laboratório de Química Orgânica e Farmacêutica, Departamento de Ciências Químicas, Faculdade de Farmácia, Universidade do Porto, Rua de Jorge Viterbo Ferreira 228, 4050-313, Porto, Portugal*
[3]*Centro de Investigação em Ciências da Saúde, Instituto Superior de Ciências da Saúde-Norte, (CICS-ISCS-N), Rua Central de Gandra 1317, 4585-116, Gandra PRD, Portugal*

ABSTRACT The resolution of seven enantiomeric pairs of chiral derivatives of xanthones (CDXs) on (*S,S*)-Whelk-O1 and L-phenylglycine chiral stationary phases (CSPs) was systematically investigated using multimodal elution conditions (normal-phase, polar-organic, and reversed-phase). The (*S,S*)-Whelk-O1 CSP, under polar-organic conditions, demonstrated a very good power of resolution for the CDXs possessing an aromatic moiety linked to the stereogenic center with separation factor and resolution factor ranging from 1.91 to 7.55 and from 6.71 to 24.16, respectively. The chiral recognition mechanisms were also investigated for (*S,S*)-Whelk-O1 CSP by molecular docking technique. Data regarding the CSP–CDX molecular conformations and interactions were retrieved. These results were in accordance with the experimental chromatographic parameters regarding enantioselectivity and enantiomer elution order. The results of the present study fulfilled the initial objectives of enantioselective studies of CDXs and elucidation of intermolecular CSP–CDX interactions. *Chirality 25:89–100, 2013.*

KEY WORDS: Pirkle-type chiral stationary phases; chiral derivatives of xanthones; enantioselectivity; chiral recognition; intermolecular interactions; docking

INTRODUCTION

Enantiomers are often readily distinguished by biological systems, presenting different pharmacokinetic and pharmacodynamic properties. Thus, chiral separation has been a major focus for analytical and organic chemistry during the last three decades being nowadays crucial for drug development process.[1] Over the years, high-performance liquid chromatography (HPLC) has emerged as one of the most useful methods for analyses and preparation of enantiomerically pure bioactive compounds.[2] The remarkable development and applications of chiral stationary phases (CSPs) have revolutionized the field of chiral separation providing both enantiomers in high enantiomeric purity, which is one of the conditions required for biological, pharmacological, or toxicological evaluations of chiral bioactive compounds.[3]

Among the most useful CSPs described in the literature is the brush-type or Pirkle-type CSPs. The selectors of these CSPs are chiral small molecules chemically bonded to silica or silica derivatives. Pirkle *et al.*[4] were the pioneers on the development of those type of CSPs, with almost a hundred CSPs reported being many of them commercially available.[5] The principle of reciprocity[6] and the chiral recognition phenomena, based on chromatographic[7,8] and spectroscopic studies,[9,10] were the centerpieces of the evolution of Pirkle-type CSPs. Pirkle et col. inspired other groups to develop numerous Pirkle-type CSPs with chiral low-molecular mass selectors,[3,11–13] including our group.[14] Among the great number of Pirkle-type CSPs described in the literature, Whelk-O1 CSP (Fig. 1a) is one of the most employed with the broadest application in industrial and academic laboratories.[5] Applying an immobilized guest strategy, this CSP has been designed in the 1990s[15] to undergo H bonding, face-to-face, and edge-to-face π–π interactions with the enantiomers of naproxen. Moreover, the Whelk-O1 CSP has also been effective for separating many others racemates[16–20] including drugs.[15,16,21,22]

The π-acceptor amino acid-derived CSP phenylglycine (Fig. 1b) was one of the first CSP developed by Pirkle *et al.*[23] Although its enantioselectivity power is lower than Whelk-O1 CSP, it was demonstrated to be useful for separation of different classes of enantiomers, such as non-steroidal anti-inflammatory drugs[24] and benzodiazepinones,[25] among others.

In recent years, the computational study of chromatographic separations has become a very important tool in understanding the chiral recognition mechanisms for diverse CSPs,[5] particularly Whelk-O1 CSP which has been investigated in detail by molecular modeling,[26,27] chemoinformatics,[28,29] and molecular simulation[30–32] studies. The elucidation of chiral recognition mechanisms is essential to clarify the kind of intermolecular interactions between each enantiomer and the CSP and may provide valuable information to estimate the magnitude of the enantioselectivity, anticipate the elution order, predict that other classes of racemates can be separated, and establish

Contract grant sponsor: This work was funded by FCT – Fundação para a Ciência e a Tecnologia under the project CEQUIMED-PEst-OE/SAU/UI4040/2011 and also by FEDER funds through the COMPETE program under the project FCOMP-01-0124-FEDER-011057.
*Correspondence to: Madalena M. Pinto, Centro de Química Medicinal da Universidade do Porto (CEQUIMED-UP), Laboratório de Química Orgânica e Farmacêutica, Departamento de Ciências Químicas, Universidade do Porto, Rua de Jorge Viterbo Ferreira 228, 4050–313 Porto, Portugal. E-mail: madalena@ff.up.pt; madalenakijjoa@gmail.com
Received for publication 14 April 2012; Accepted 04 August 2012
DOI: 10.1002/chir.22112
Published online 10 December 2012 in Wiley Online Library (wileyonlinelibrary.com).

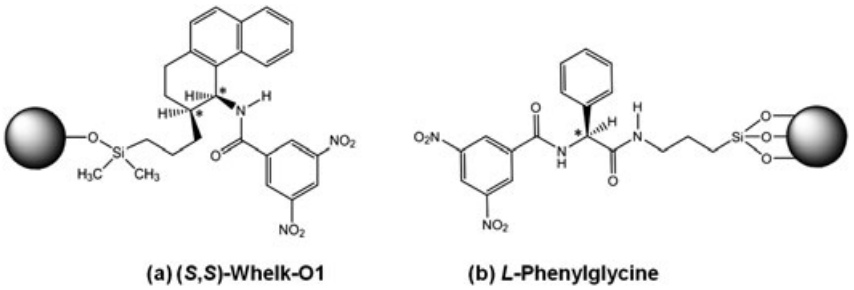

Fig. 1. The chemical structures of (a) (*S*,*S*)-Whelk-O1 and (b) L-phenylglycine CSPs.

the more suitable chromatographic conditions. Moreover, it is also useful to guide structural modifications of the molecules of the CSPs in order to obtain a higher enantiomeric selectivity for a specific class of enantiomers.

The importance of xanthone derivatives is well recognized in medicinal chemistry concerning their broad spectrum of biological and pharmacological activities.[33–36] Our group has been active in synthesizing compounds based on the xanthonic scaffold for biological activity evaluation,[34–40] including chiral derivatives.[14,40] In the literature, chiral derivatives of xanthones (CDXs) have been reported to reveal antitumoral,[40] antifungal, and antibacterial,[41] antiepileptic and anticonvulsant[42–45] antiarrhythmic,[46] and local anesthetic[45] activities, among others.

Herein, we describe an investigation of the resolution of seven enantiomeric pairs of CDXs (Fig. 2) on (*S*,*S*)-Whelk-O1 and L-phenylglycine CSPs. Besides that, this work explores the influence of different mobile phases on enantiomeric separation. So, multimodal elution conditions: normal-phase, polar-organic, and reversed-phase modes were explored on both CSPs.

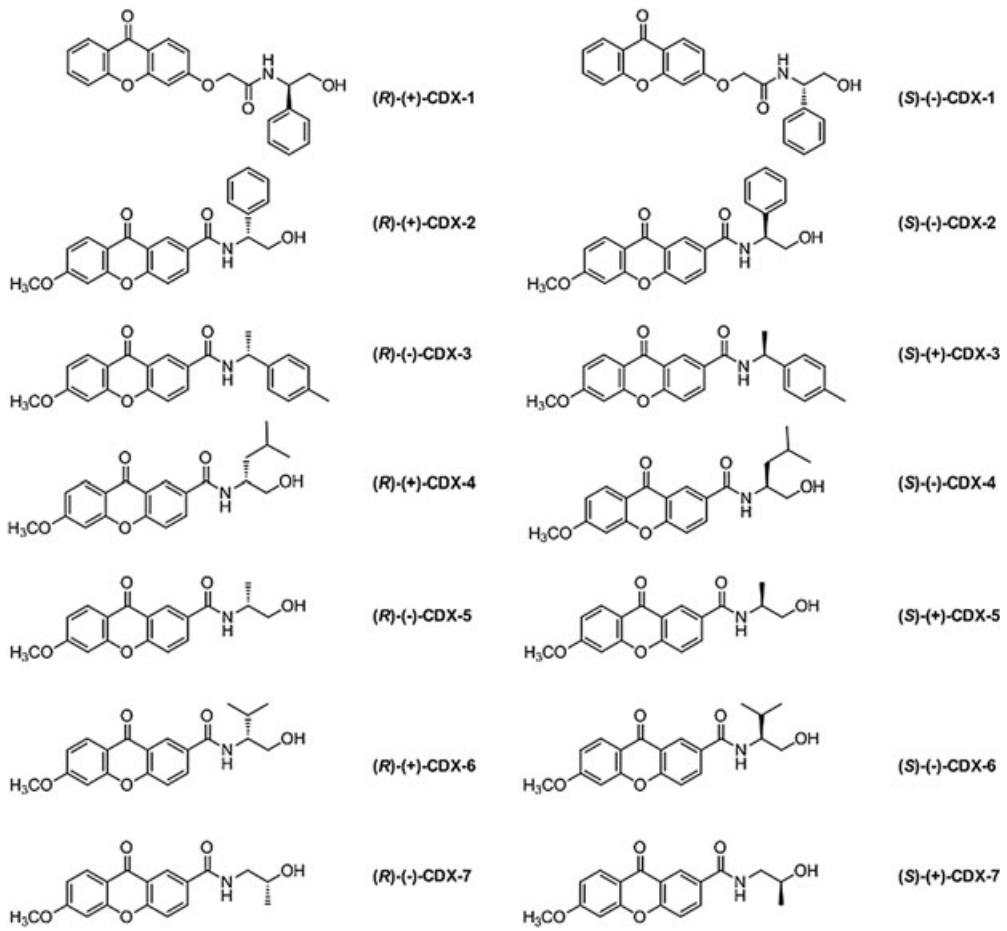

Fig. 2. The chemical structures of enantiomeric pairs of CDXs: (*R*)-(+) and (*S*)-(−)-**CDX-1** (*N*-(2-hydroxy-1-phenylethyl)-2-((9-oxo-9*H*-xanthen-3-yl)oxy)acetamide); (*R*)-(+) and (*S*)-(−)-**CDX-2** (*N*-(2-hydroxy-1-phenylethyl)-6-methoxy-9-oxo-9*H*-xanthene-2-carboxamide); (*R*)-(−) and (*S*)-(+)-**CDX-3** (6-methoxy-9-oxo-*N*-(1-(*p*-tolyl) ethyl)-9*H*-xanthene-2-carboxamide); (*R*)-(+) and (*S*)-(−)-**CDX-4** (*N*-(1-hydroxy-4-methylpentan-2-yl)-6-methoxy-9-oxo-9*H*-xanthene-2-carboxamide); (*R*)-(−) and (*S*)-(+)-**CDX-5** (*N*-(1-hydroxypropan-2-yl)-6-methoxy-9-oxo-9*H*-xanthene-2-carboxamide); (*R*)-(+) and (*S*)-(−)-**CDX-6** (*N*-(1-hydroxy-3-methylbutan-2-yl)-6-methoxy-9-oxo-9*H*-xanthene-2-carboxamide); and (*R*)-(−) and (*S*)-(+)-**CDX-7** (*N*-(2-hydroxypropyl)-6-methoxy-9-oxo-9*H*-xanthene-2-carboxamide).

Based on chromatographic data obtained on (*S*,*S*)-Whelk-O1 CSP, docking studies were performed in order to better understand the chromatographic behavior at a molecular level, as well as the structural features associated with the chiral recognition mechanism.

The enantiomeric resolution of the same library of enantiomeric pairs of CDXs using four macrocyclic antibiotic CSPs under multimodal elution conditions as well as the chiral recognition mechanisms by docking studies was recently demonstrated.[47] Regarding the enantiomeric pairs of CDXs and comparing the enantioselectivity on both type of CSPs, this work confirms that (*S*,*S*)-Whelk-O1, L-phenylglycine, and macrocyclic antibiotic CSPs reveal a distinct pattern of enantioselectivity.

To our best knowledge, this is the first report of the use of (*S*,*S*)-Whelk-O1 and L-phenylglycine CSPs for the enantioseparation of this important class of compounds.

MATERIALS AND METHODS

Chemicals

The procedures to synthesize the CDXs (Fig. 2) were described elsewhere.[14] Briefly, carboxyxanthone derivatives were coupled with both enantiomers of commercially available chiral building blocks using *O*-(benzotriazol-1-yl)-*N*,*N*,*N*′,*N*′-tetramethyluronium tetrafluoroborate as coupling reagent. Ethanol (EtOH), 2-propanol (2-prOH), *n*-hexane (Hex), methanol (MeOH), and acetonitrile (ACN) HPLC grade were purchased from Sigma-Aldrich Co (St. Louis, MO, USA). Ultrapure water was produced by a Millipore Milli-Q system (Millipore, Bedford, MA, USA). The stock solutions of the CDXs were prepared by dissolution in EtOH at the concentration of 0.5 mg/ml. Working solutions of enantiomeric pairs of CDXs were prepared by mixing equal aliquots of each enantiomer.

Chromatography

The HPLC system was a JASCO model 880-PU pump, a Rheodyne model 7125 injector fitted with a 20-µl sample loop, a JASCO model 880-30 solvent mixer, and a JASCO model 875-UV detector (Tokyo, Japan). A DataApex CSW17 - chromatography station for Microsoft Windows 95 was employed. The chiral columns (*S*,*S*)-Whelk-O1 and L-phenylglycine (25 cm × 4.6 mm i.d., 5-µm particle size, 100-Å pore size) were commercially available from Regis Technologies, Inc. (Morton Grove, IL, USA). Analyses were performed at room temperature in isocratic mode using multimodal conditions. The mobile phase compositions were Hex and EtOH or 2-prOH as a modifier, in normal-phase condition; MeOH and water were used in reversed-phase condition. MeOH, EtOH, ACN, or mixtures with different proportions of these solvents were used in polar-organic elution conditions. The mobile phases were prepared in a volume/volume relation and degassed in an ultrasonic bath for 15 min before use. The flow rate used was 1.0 ml/min, and the chromatograms were monitored by ultraviolet detection at a wavelength of 254 nm. The measurements were carried out at the laboratory temperature (22 ± 2 °C). The sample injections (20 µl) were carried out in triplicate. The dead time (t_0) was considered to be equal to the peak of the solvent front and was taken from each particular run. The retention factor (k) was calculated using the equation ($k = [t_R - t_0]/t_0$). The separation factor (α) was calculated as ($\alpha = k_2/k_1$). The resolution factor (R_s) was calculated using the equation ($R_s = 1.18\ [t_{R2} - t_{R1}]/[W_{1\ 0.5} + W_{2\ 0.5}]$) where t_{R1} and t_{R2} are the retention times of the first and second enantiomers, respectively, and $W_{1\ 0.5}$ and $W_{2\ 0.5}$ are the corresponding peak width measured on half height. The elution order was determined for the enantiomers of CDXs **1–3** on (*S*,*S*)-Whelk-O1 CSP by injecting the solutions of the enantiomeric mixtures and then each enantiomer separately, using ACN : MeOH (50:50 v/v) and with only MeOH as mobile phases.

Computational

The (*S*,*S*)-Whelk-O1 selector was retrieved from the Cambridge Crystallographic Data Centre (deposition number 273851), and it is based on previous X-ray crystallographic studies.[48,49] The docking simulations were done considering only the structural features which are assumed to be essential for enantioselectivity. For this study, the support (silica) and the spacer were replaced by a methyl group. The CDXs were subject to energy minimization by using HyperChem version 8.0.[50] The semi-empirical Austin Model 1[51] method with the Polak–Ribière algorithm was employed for molecular minimization. Docking simulations between the CDXs and the (*S*,*S*)-Whelk-O1 selector were undertaken in AutoDock Vina[52] embedded in PyRx–Virtual Screening Tool software, release 0.8 for Windows. AutoDock Vina considered the target conformation (selector) as a rigid unit, whereas the ligands (CDXs) were allowed to be flexible and adaptable to the target. Vina searched for the lowest binding affinity conformations and returned nine different conformations for each CDX. AutoDock Vina was run using an exhaustiveness of eight and a grid box with the dimensions 13.0, 13.0, and 10.0, engulfing the entire selector. Conformations and interactions were visualized using PyMOL version 1.3.[53]

To position explicit solvent (MeOH) in the binding site, AutoDock Vina[52] was used to obtain the top-scoring poses using the previously described protocol. The selector plus MeOH was used as "receptor" in a new docking study using CDXs **1–7** as potential ligands.

AutoDock 4 implemented in AutoDockTools was used to dock CDXs **1–7** into flexible (*S*,*S*)-Whelk-O1. Amide bond between dinitrophenyl group and 1,2,3,4-tetrahydrophenanthrene group was defined as flexible. A three-dimensional grid box of 13.0, 13.0, and 10.0 (x,y,z) that encompassed the selector cleft was defined. AutoDock 4 was used to dock CDXs **1–7** to the selector, and each structure was scored and ranked.

RESULTS AND DISCUSSION

The Whelk-O1 CSP has been designed mainly to operate under normal-phase HPLC conditions. However, the Whelk-O1 CSP has also been reported to be useful in polar-organic and reversed-phase elution conditions, within a wide range of mobile phases.[16,22,54,55] Indeed, recent publications are devoted to the adsorption of naproxen on Whelk-O1 CSP under reversed-phase conditions,[56,57] concerning the effect of mobile phase[58] and buffer composition.[59] As a general rule, enantiomers that exhibit an H-bond acceptor and an aromatic moiety close to the stereogenic center tend to be well resolved on Whelk-O1 CSP.[16] L-Phenylglycine CSP has also been proven to be capable to operate not only under normal-phase elution conditions but also reversed-phase conditions.[24] Hence, the enantioresolution of seven enantiomeric pairs of CDXs (**1–7**) (Fig. 2) was evaluated on (*S*,*S*)-Whelk-O1 and L-phenylglycine CSPs (Fig. 1), under normal-phase, polar-organic, and reversed-phase elution conditions.

Performance of (S,S)-Whelk-O1 CSP for Resolution of CDXs

Three out of seven enantiomeric pairs of CDXs (**1–3**) were enantioseparated with excellent enantioselectivity on (*S*,*S*)-Whelk-O1 CSP, with α ranging from 1.91 to 7.55 and resolutions ranging from 6.71 to 24.16. The overall best results are shown on Table 1.

Briefly, under the normal-phase elution conditions using EtOH as the modifier, very high retention factors were observed with low percentage of the modifier, being the chromatographic run up to 120 min. In order to overcome this situation, the polarity of the mobile phase was increased to consequently decrease the retention time of the enantiomers. Thus, the EtOH : Hex mobile phase was evaluated systematically, changing the content of EtOH from 10% to 90% (by volume) in increments of 10% each time (data not shown). Meanwhile, with EtOH : Hex (90:10 v/v), excellent enantioselectivity and resolution were achieved for the enantiomeric pairs of CDXs **1–3**, with $\alpha = 2.99$, 4.25, and

TABLE 1. Separation performance of (*S*,*S*)-Whelk-O1 CSP, under multimodal chromatographic conditions, for the enantiomeric pairs of CDXs (1–3)

	CDX-1				CDX-2				CDX-3			
Mobile phase	k_1	k_2	α	R_s	k_1	k_2	α	R_s	k_1	k_2	α	R_s
EtOH/Hex: 90/10	2.51	7.50	2.99	10.78	1.94	8.24	4.25	13.17	2.59	19.58	7.55	17.58
EtOH	2.30	6.73	2.93	10.05	1.84	7.57	4.11	12.14	2.58	18.58	7.21	16.15
MeOH	1.36	3.08	2.27	10.63	1.28	3.55	2.78	12.77	1.98	9.95	5.02	22.04
ACN	1.03	2.11	2.06	8.16	1.21	3.22	2.66	10.29	1.24	6.82	5.50	24.16
ACN/MeOH: 50/50	0.64	1.14	1.91	6.71	0.60	1.41	2.47	8.85	0.91	3.61	4.08	19.46
MeOH/H_2O: 80/20	9.09	22.44	2.47	13.14	7.04	7.04	1.00	–	16.21	16.21	1.00	–

CSP, chiral stationary phase; CDX, chiral derivative of xanthone; EtOH, ethanol; Hex , *n*-hexane; MeOH, methanol; ACN, acetonitrile.

7.55 and R_S = 10.78, 13.17, and 17.58, respectively (Table 1). However, with this mobile phase, the retention factors of the second eluted enantiomer were still very high (k_2 ranging from 7.50 to 19.58), leading to a high analysis time. Therefore, to overcome this situation, the strategy was using only EtOH as mobile phase (polar-organic elution conditions). Nevertheless, when EtOH was used as mobile phase, the results were similar as those described for EtOH : Hex (90:10 v/v). So, the uses of other polar-organic solvents were attempted by switching to MeOH and ACN as mobile phases. Lower retention factors were observed when changing from EtOH to MeOH or ACN (Fig. 3), whereas the enantioselectivity and resolution are at a standstill excellent (Fig. 4). Moreover, the mixtures of two polar-organic solvents as ACN and MeOH (50:50 v/v) allowed shortened retention factors of both enantiomers of CDXs **1–3**, when compared to 100% MeOH or ACN as mobile phase (Fig. 3). Actually, when a mixture of ACN : MeOH (50:50 v/v) was used, the enantioselectivity and resolutions decreased only slightly (Fig. 4); however, the overall chromatographic parameters were excellent. Figure 5 compares characteristic chromatograms with different mobile phases, with ACN : MeOH (50:50 v/v) presenting the best performance.

Finally, on the reversed-phase elution conditions, very high retention factors were achieved for the enantiomeric pairs of CDXs **1–3** (Table 1). When MeOH : H_2O (80:20 v/v) was used as mobile phase, only the enantiomeric pair of **CDX-1** was baseline separated.

Considering enantiomeric pairs of CDXs **4–7**, the results were not satisfactory on (*S*,*S*)-Whelk-O1 CSP (data not shown). However, using acetonitrile as mobile phase, the enantiomeric pair of **CDX-4** was slightly separated (α = 1.10), although with poor resolution (R_S = 0.61). Similarly, the enantiomeric pair of **CDX-5** was only partially resolved with MeOH : H_2O

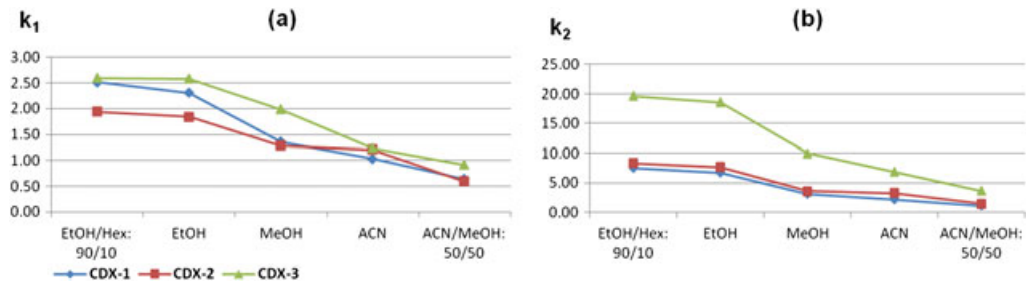

Fig. 3. Comparison of retention factors of the (**a**) first enantiomer (k_1) and (**b**) the second enantiomer (k_2) of (♦) **CDX-1**, (■) **CDX-2**, and (▲) **CDX-3** on (*S*,*S*)-Whelk-O1 CSP under normal-phase and polar-organic elution conditions; flow rate 1.0 ml/min; detection wavelength 254 nm.

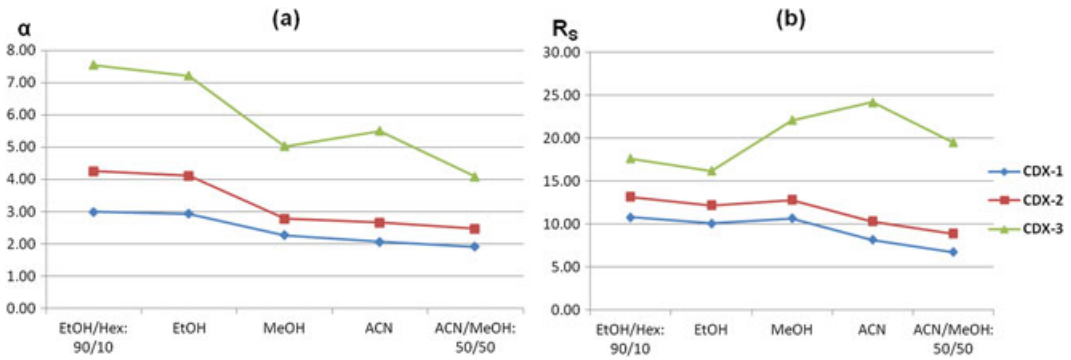

Fig. 4. Comparison of (**a**) enantioselectivity (α) and (**b**) resolution (R_S) of (♦) **CDX-1**, (■) **CDX-2**, and (▲) **CDX-3** on (*S*,*S*)-Whelk-O1 CSP under normal-phase and polar-organic elution conditions; flow rate 1.0 ml/min; detection wavelength 254 nm.

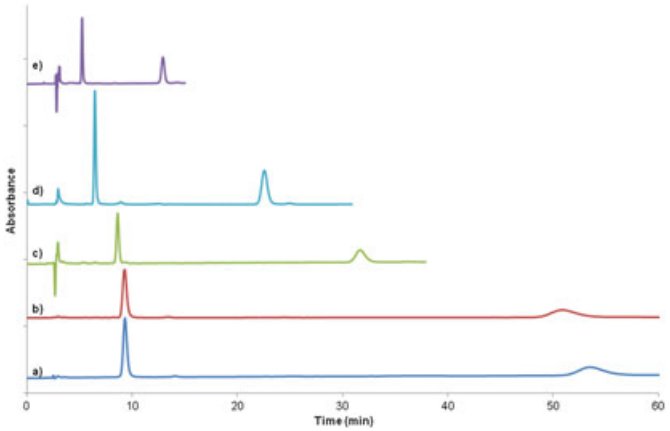

Fig. 5. Chromatograms of enantiomeric pair of **CDX-3** on (*S*,*S*)-Whelk-O1 CSP in the mobile phases (a) EtOH : Hex (90:10 v/v), (b) EtOH, (c) MeOH, (d) ACN, and (e) ACN : MeOH (50:50 v/v); flow rate 1.0 ml/min; detection wavelength 254 nm.

TABLE 2. Separation performance of L-phenylglycine CSP, under multimodal chromatographic conditions, for the enantiomeric pair of CDX-3

	CDX-3		
Mobile phase	k_1	α	R_s
EtOH/Hex: 25/75	5.26	1.24	2.51
EtOH/Hex: 40/60	2.80	1.23	2.08
EtOH/Hex: 50/50	2.26	1.23	1.90
2-PrOH/Hex: 50/50	4.87	1.35	1.60
EtOH	0.92	1.21	1.24
MeOH	0.64	1.16	1.13
ACN	0.51	1.21	0.66
ACN/MeOH: 50/50	0.22	1.00	–
MeOH/H_2O: 80/20	4.54	1.19	1.71

CSP, chiral stationary phase; CDX, chiral derivative of xanthone; EtOH, ethanol; Hex, *n*-hexane; 2-PrOH, 2-propanol; MeOH, methanol; ACN, acetonitrile.

(80:20 v/v), also with poor enantioselectivity (α = 1.06) and resolution (R_S = 0.76). The enantiomeric pairs of **CDX-6** and **CDX-7** were not separated, under all the chromatographic elution conditions evaluated.

Thus, as predicted for (*S*,*S*)-Whelk-O1,[16] the chromatographic results demonstrated that the best resolved enantiomeric pairs of CDXs were the ones that, in addition to an H-bond acceptor, have also an aromatic moiety next to the stereogenic center, i.e., CDXs **1–3** (Fig. 2). In spite of the fact that, for these xanthonic enantiomeric pairs, the best enantioselectivity and resolution were achieved using EtOH : Hex (90:10 v/v) as mobile phase (Table 1), polar-organic conditions proved to be a best alternative to the normal-phase conditions, since lower retention factors with high enantioselectivity and resolution were obtained when ACN : MeOH (50:50 v/v) was used as mobile phase, indicating that this might be preferable for faster analytical separations.

The elution order for the enantiomers of CDXs **1–3** using either MeOH or ACN : MeOH (50:50 v/v) as mobile phase demonstrated that the (*S*)-enantiomer of pairs of CDXs **1–2** was the first to elute, whereas for **CDX-3**, the (*S*)-enantiomer was the more retained.

Performance of L-Phenylglycine CSP for Resolution of CDXs

The capability of L-phenylglycine CSP to resolve the CDXs series was also systematically evaluated under multimodal elution conditions. However, the L-phenylglycine CSP showed much lower discrimination capability for the enantiomeric pairs of CDXs evaluated compared to (*S*,*S*)-Whelk-O1 CSP. In fact, enantiomeric pair of **CDX-3** was the only pair resolved on this CSP. Indeed, under normal elution conditions, the L-phenylglycine CSP was found to be very effective for the enantioseparation of enantiomeric pair of **CDX-3** using EtOH : Hex (25:75 v/v) as mobile phase with enantioselectivity and resolution of α = 1.24 and R_S = 2.51, respectively (Table 2). When EtOH was used in a 40% or 50% proportion in Hex, enantioresolution was decreased, with R_S = 2.08 and 1.90, respectively.

In an attempt to optimize the mobile phase composition, 2-PrOH was evaluated as an organic modifier. The enantioselectivity (α = 1.35) was improved, but the resolution was decreased (R_S = 1.60), when 2-PrOH : Hex (50:50 v/v) was used. In spite of the fact that polar-organic mode was the most successful elution condition on (*S*,*S*)-Whelk-O1 CSP (Table 1), on L-phenylglycine CSP, the poorest results were obtained with only polar-organic solvents, with α 1.21 and R_S 1.24 (Table 2). Finally, good enantioselectivity (α = 1.19) and resolution (R_S = 1.71) were obtained on reversed-phase elution condition, using MeOH : H_2O (80:20 v/v) as mobile phase, although with high retention (k_1 = 4.54). Characteristic chromatograms showing the separation performance of L-phenylglycine CSP, under normal-phase and polar-organic elution conditions, for the enantiomeric pair of **CDX-3** are depicted in Figure 6.

The enantiomeric pairs of CDXs **1–2** and **4–7** were not separated, under all the chromatographic elution conditions tested, and in general, high retentions were observed (data not shown).

Comparing the differences among the structures of the CDXs, it can be seen that **CDX-3** is the only one that has no primary alcoholic group linked to the stereogenic center. Concerning all these features, it can be inferred that this group might be responsible for strong and not enantioselective interactions for enantiomeric pairs of CDXs **1–2** and **4–7**.

Docking Studies

Comparing the major structural differences between the two Pirkle-type CSPs evaluated, the (*S*,*S*)-Whelk-O1 CSP has a semi-rigid framework (cleft type) formed by an

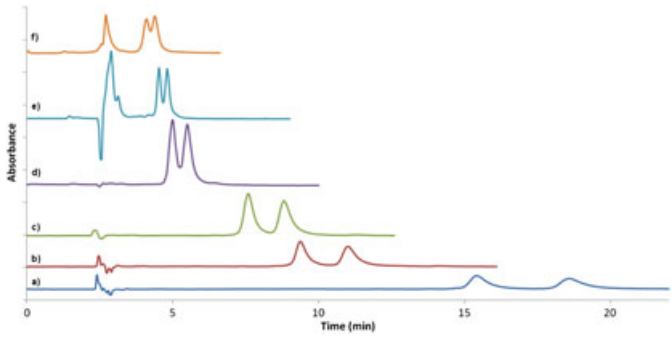

Fig. 6. Chromatograms of enantiomeric pair of **CDX-3** on L-phenylglycine CSP in the mobile phases (a) EtOH : Hex (25:75 v/v), (b) EtOH : Hex (40:60 v/v), (c) EtOH : Hex (50:50 v/v), (d) EtOH, (e) MeOH, and (f) ACN; flow rate 1.0 ml/min; detection wavelength 254 nm.

electron-deficient 3,5-dinitrophenyl group, spatially oriented in a perpendicular way to an electron-rich phenanthryl group, as well as an amide H in the cleft formed by the two aromatic systems.[16] Accordingly, it should be noted that the semi-rigid selector of the (*S*,*S*)-Whelk-O1 CSP may be crucial for the enantioresolution of this important class of compounds as an artificial "active site" for chiral recognition.

Considering the structural features of the (*S*,*S*)-Whelk-O1 selector, three simultaneous interactions were proposed by Pirkle *et al*.: an H-bonding interaction between the amide hydrogen of the selector and an H acceptor in the enantiomer; a face-to-face π–π interaction between the 3,5-dinitrophenyl group of the selector and an aromatic moiety in the enantiomer; and an edge-to-face π–π interaction between the phenanthryl group of the selector and an aromatic moiety in the enantiomer.[16] However, several studies demonstrated that the details of interactions between enantiomers and Whelk-O1 CSP can be more diverse and complex than this simple three-point model.[27,31]

The CDXs used in this study share a common structural xanthonic scaffold, with a methoxyl group at position 6, linked by an amide bond as a chemical bridge to a chiral moiety. An exception is **CDX-1** in which the xanthonic scaffold has no methoxyl group, and the link to the chiral moiety is through an ether chemical bridge (Fig. 2). The major structural differences for these molecules are in the nature of the chiral moiety, namely, a phenyl ring linked to the stereogenic center, in CDXs **1–3**. Thus, it is expectable that these molecular features might be determining for enantiorecognition on (*S*,*S*)-Whelk-O1 CSP, specifically the phenyl ring next to the stereogenic center, since the intermolecular interactions related to this group are crucial for the chiral recognition mechanism on this Pirkle-type CSP.[16] Moreover, several molecular interactions might occur with the CSP such as π–π and H bonding with the xanthonic scaffold, H bonding with the polar sites of the chiral moiety, and as well as π–π interactions with the phenyl ring (CDXs **1–3**). Besides, not only the structures of the CDXs and the CSP suggest that π–π and H-bonding interactions play an important role but also the chromatographic results achieved under normal-phase and polar-organic conditions contribute to this conclusion.

In order to elucidate the chiral recognition mechanisms of CDXs on (*S*,*S*)-Whelk-O1 CSP, all the enantiomeric pairs were used to perform computational simulations using AutoDock Vina.[52,60] The docking simulations produced nine docked conformations for each CDX. The values of binding affinity for the best scoring, i.e., the lowest binding affinity conformation, for each CDX are displayed in Table 3. Energy difference values were calculated as the difference in energy of the lowest binding affinity conformation of (*R*)-CDX-CSP complex versus (*S*)-CDX-CSP complex.

The PyRx/AutoDock Vina calculations lead to a successful reproduction of the enantioselectivity for all enantiomeric pairs of CDXs, whereas only an 86% of accordance was obtained concerning elution order. Accordingly, regarding enantiomeric pair of **CDX-2**, the more retained enantiomer, (*R*)-(+)-**CDX-2**, binds to the (*S*,*S*)-Whelk-O1 selector with higher affinity, i.e., lower binding energy (−6.2 kcal/mol), compared to the first eluted enantiomer (−5.3 kcal/mol). Concerning enantiomeric pair of **CDX-3**, there is also an energetic difference between each enantiomer–CSP complex: the (*S*)-enantiomer binds to the chiral selector with higher affinity (−6.1 kcal/mol) than the (*R*)-enantiomer (−4.7 kcal/mol). The computational calculations confirmed the experimental chromatographic data, since (*S*)-(+)-**CDX-3** was the more retained enantiomer.

Furthermore, the calculated binding affinities differences between the enantiomers of the same enantiomeric pair of CDXs are also directly related with the magnitude of the experimental separation factors (except enantiomeric pair of **CDX-1**). For example, the enantiomeric pair of **CDX-3** has the highest energy difference (1.4 kcal/mol) and also the highest enantioselectivity ($\alpha = 4.08$). Finally, considering enantiomeric pairs of CDXs **4–7**, low separation factors (1.00 to 1.10) are in agreement with the low docking energy difference (0 to −0.5). For example, the binding energies are equal for both enantiomers of **CDX-7** (−5.1 kcal/mol) indicating that they have identical affinity for the (*S*,*S*)-Whelk-O1 selector, which is in accordance with the chromatographic results at any elution conditions attempted (no separation was achieved, $\alpha = 1.00$).

Interestingly, the enantiomeric pair of **CDX-1** was the only pair which the order of elution obtained by docking studies

TABLE 3. Calculated binding energy values of the lowest binding affinity conformation for each enantiomer of CDXs 1–7

CDX	Binding affinity (kcal/mol)	Energy difference (kcal/mol)	Elution order	α
(*R*)-(+)-**CDX-1**	−4.5	1.4	Second	1.91
(*S*)-(−)-**CDX-1**	−5.7		First	
(*R*)-(+)-**CDX-2**	−6.2	−0.9	Second	2.47
(*S*)-(−)-**CDX-2**	−5.3		First	
(*R*)-(−)-**CDX-3**	−4.7	1.4	First	4.08
(*S*)-(+)-**CDX-3**	−6.1		Second	
(*R*)-(+)-**CDX-4**	−5.5	−0.5	–	1.10
(*S*)-(−)-**CDX-4**	−5.0		–	
(*R*)-(−)-**CDX-5**	−5.4	−0.2[1]	–	1.06
(*S*)-(+)-**CDX-5**	−5.2		–	
(*R*)-(+)-**CDX-6**	−5.2	−0.2[1]	–	1.00
(*S*)-(−)-**CDX-6**	−5.0		–	
(*R*)-(−)-**CDX-7**	−5.1	0.0	–	1.00
(*S*)-(+)-**CDX-7**	−5.1		–	

CDX, chiral derivative of xanthone.
[1]Energy differences not considered significant.

was found to be the opposite of the experimental data. Comparing the differences among the structures of the CDXs, it can be seen that the substituent and its position on the xanthonic scaffold were different on **CDX-1**. These structural features and the limitations associated with the stochastic docking algorithms may justify this incorrect docking calculation.

The docked conformations with the lowest binding energy of each enantiomer of CDXs **2–3** and **7** are demonstrated in Figures 7–9, respectively. The selection includes two enantiomeric pairs of CDXs which were resolved with very high R_s values, **CDX-2** and **CDX-3** (Table 1), and one enantiomeric pair without any degree of resolution under any elution condition, **CDX-7**.

Figure 7 demonstrates that both enantiomers of **CDX-2** interact inside the cleft of the (*S*,*S*)-Whelk-O1 selector. However, the superimposition of (*R*) and (*S*) enantiomers (Fig. 7a) shows that their positions are not similar. Contrary to (*S*)-enantiomer, it must be noted that the (*R*)-(+)-**CDX-2** adopts a conformation where the xanthonic scaffold lies parallel to the phenanthryl group of the selector as well as the phenyl ring relatively to the dinitrophenyl group of the selector. So, the π–π interactions between these aromatic rings may be stronger for this enantiomer (Fig. 7d), compared to (*S*)-enantiomer (Fig. 7e). Another difference is the position of the NH amide of the chiral moiety, which is inside the cleft for (*R*)-enantiomer and outside for (*S*)-enantiomer. So, the (*R*)-(+)-**CDX-2** can establish an H-bonding interaction with a nitro oxygen of a dinitrophenyl group of the selector (Fig. 7b). However, this H-acceptor group of the selector also establishes an H-bonding interaction with the *S*-enantiomer, but with the H-donor hydroxyl group of the chiral moiety (Fig. 7c). Additionally, both enantiomer–CSP complexes display H-bonding interactions between the xanthonic carbonyl group and NH amide of the selector.

Concerning the enantiomeric pair of **CDX-3**, it is important to highlight that each enantiomer interacts in a very different way with the (*S*,*S*)-Whelk-O1 selector: whereas the less retained enantiomer, (*R*)-(−)-**CDX-3**, interacts with the selector in a more outward position in the cleft, the more retained enantiomer, (*S*)-(+)-**CDX-3**, docks on the opposite side of the dinitrophenyl group, in a more inward position (Fig. 8a). Thus, these differences are decisive for the chiral recognition mechanism. Figure 8 demonstrated that both enantiomers of **CDX-3** establish one H bonding and two π–π interactions with the chiral selector. However, the functional groups implicated on the interactions are not the same. Accordingly, the NH amide of the selector forms an H-bonding interaction with the oxygen of the xanthonic heterocycle ring of the (*S*)-(+)-**CDX-3** (Fig. 8b), whereas the H-bond acceptor of (*R*)-(−)-**CDX-3** is the xanthonic carbonyl group (Fig. 8c). Additionally, for (*S*)-(+)-**CDX-3**, two π–π interactions are established: one with the xanthonic scaffold and the dinitrophenyl group of the selector, and another with the phenyl ring, bonded to the stereogenic center, and the phenanthryl group of the selector (Fig. 8d). Contrary to (*S*)-enantiomer, the xanthonic scaffold of (*R*)-(−)-**CDX-3** establishes a π–π interaction with the phenanthryl group of the selector, and the phenyl ring establishes a π–π interaction with dinitrophenyl group of the selector (Fig. 8e).

Concerning enantiomeric pair of **CDX-7**, both enantiomers adopt similar conformations inside the cleft of the (*S*,*S*)-Whelk-O1 selector (Fig. 9a). They also establish similar intermolecular interactions, namely, H bonding

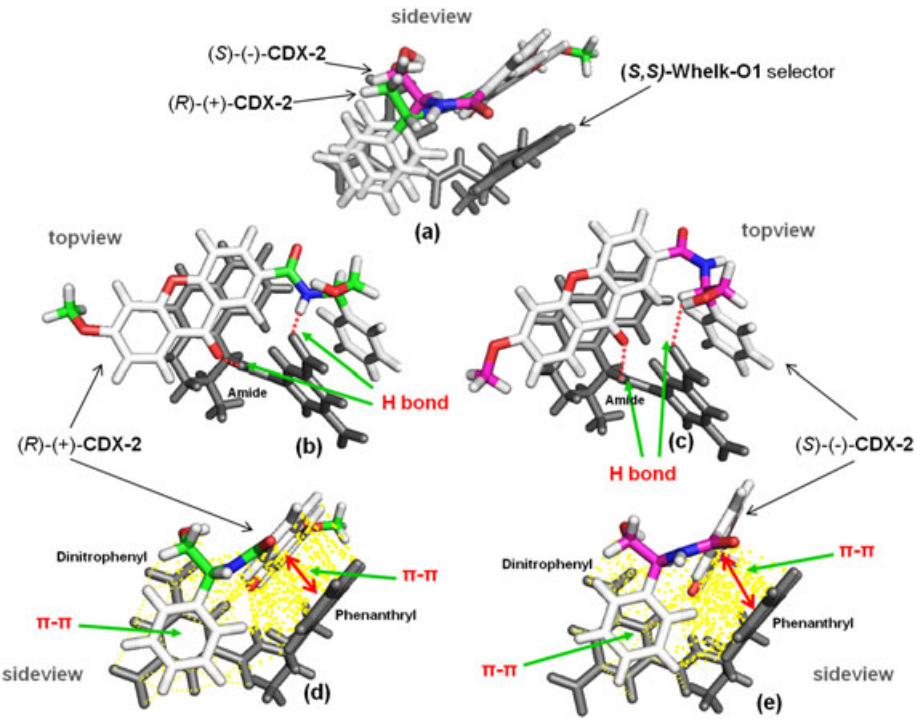

Fig. 7. The most stable docked conformations of both enantiomers of **CDX-2** complexed to (*S*,*S*)-Whelk-O1 selector (gray): (**a**) superimposed CDX–CSP complexes, H-bonding interactions of (**b**) (*R*)-(+)-**CDX-2** and (**c**) (*S*)-(−)-**CDX-2**, and π–π interactions of (**d**) (*R*)-(+)-**CDX-2** and (**e**) (*S*)-(−)-**CDX-2**.The non-aromatic carbon atoms of (*R*)-(+)-**CDX-2** and of (*S*)-(−)-**CDX-2** are represented in green and purple, respectively; red dashes represent H-bonding interactions; yellow dashes represent all the other interactions; π–π interactions are highlighted with a red double edge arrow.

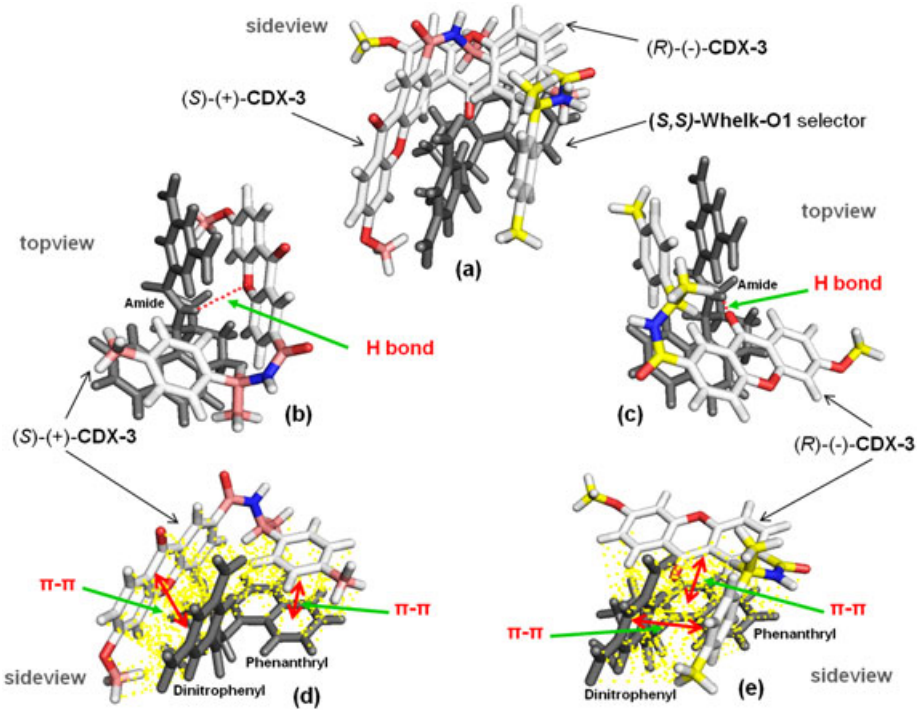

Fig. 8. The most stable docked conformations of both enantiomers of **CDX-3** complexed to (*S*,*S*)-Whelk-O1 selector (gray): (**a**) superimposed CDX–CSP complexes, H-bonding interactions of (**b**) (*S*)-(+)-**CDX-3** and (**c**) (*R*)-(−)-**CDX-3**, and π–π interactions of (**d**) (*S*)-(+)-**CDX-3** and (**e**) (*R*)-(−)-**CDX-3**.The non-aromatic carbon atoms of (*S*)-(+)-**CDX-3** and of (*R*)-(−)-**CDX-3** are represented in pink and yellow, respectively; red dashes represent H-bonding interactions; yellow dashes represent all the other interactions; π–π interactions are highlighted with a red double edge arrow.

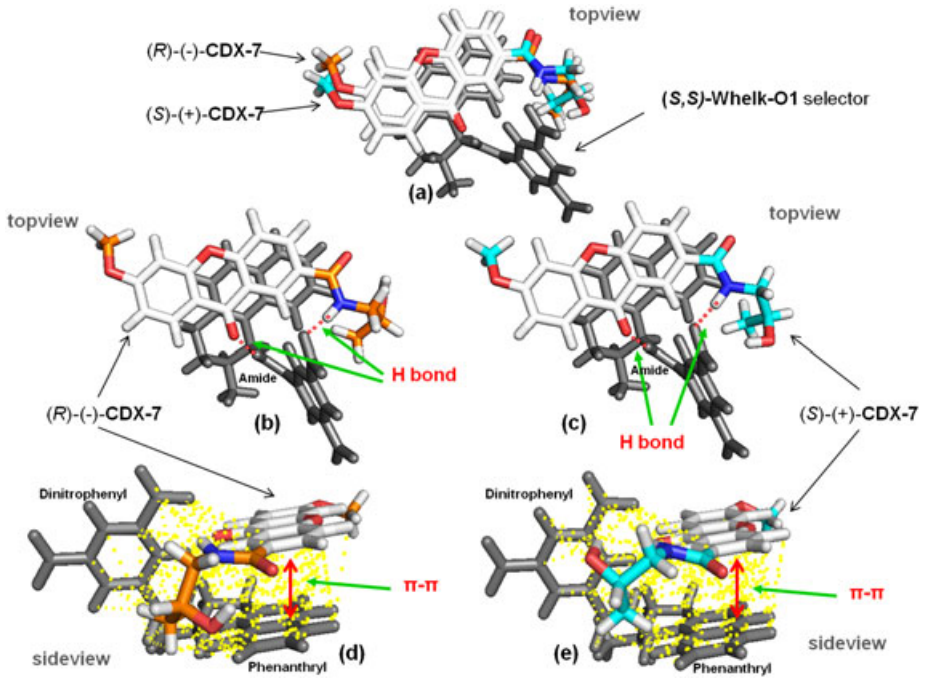

Fig. 9. The most stable docked conformations of both enantiomers of **CDX-7** complexed to (*S*,*S*)-Whelk-O1 selector (gray): (**a**) Superimposed CDX–CSP complexes, H-bonding interactions of (**b**) (*R*)-(−)-**CDX-7** and (**c**) (*S*)-(+)-**CDX-7**, and π–π interactions of (**d**) (*R*)-(−)-**CDX-7** and (**e**) (*S*)-(+)-**CDX-7**.The non-aromatic carbon atoms of (*R*)-(−)-**CDX-7** and of (*S*)-(+)-**CDX-7** are represented in orange and cyan, respectively; red dashes represent H-bonding interactions; yellow dashes represent all the other interactions; π–π interactions are highlighted with a red double edge arrow.

between the xanthonic carbonyl oxygen and the NH amide of the selector. H bonding between the NH amide of CDXs and a nitro group of the selector (Fig. 9b and c), and π–π interaction between the xanthonic scaffold and the (*S*,*S*)-Whelk-O1 phenanthryl group (Fig. 9d and e). As anticipated by the absence of chromatographic enantioselectivity, none of these interactions is stereochemically dependent.

TABLE 4. H bonding and π–π interactions statistics for the (*S,S*)-Whelk-O1 selector

	H-bonding interaction with		π–π interaction with	
Analyte	Amide hydrogen[1]	Nitro oxygen[2]	Phenanthryl	Dinitrophenyl
(*R*)-(+)-**CDX-1**	4	1	7	0
(*S*)-(−)-**CDX-1**	2	4	8	4
(*R*)-(+)-**CDX-2**	6	3	5	5
(*S*)-(−)-**CDX-2**	6	2	5	4
(*R*)-(−)-**CDX-3**	5	0	6	4
(*S*)-(+)-**CDX-3**	2	0	5	8
(*R*)-(+)-**CDX-4**	5	2	7	0
(*S*)-(−)-**CDX-4**	4	2	4	1
(*R*)-(−)-**CDX-5**	5	1	7	0
(*S*)-(+)-**CDX-5**	4	2	6	0
(*R*)-(+)-**CDX-6**	6	3	8	1
(*S*)-(−)-**CDX-6**	5	2	9	0
(*R*)-(−)-**CDX-7**	5	1	7	1
(*S*)-(+)-**CDX-7**	4	1	6	3
Total	63	24	90	31

CDX, chiral derivative of xanthone.
[1]The amide oxygen did not form any H-bonding interaction.
[2]H-bonding interactions only formed with the nitro oxygen facing the interior of the cleft.

TABLE 5. Calculated binding energy values of the lowest binding affinity conformation for each enantiomer of CDXs 1–7 on solvated[1] (*S,S*)-Whelk-O1

CDX	Binding affinity (kcal/mol)	Energy difference (kcal/mol)	Elution order	α
(*R*)-(+)-**CDX-1**	−5.3	−0.3	Second	2.27
(*S*)-(−)-**CDX-1**	−5.0		First	
(*R*)-(+)-**CDX-2**	−6.0	−0.8	Second	2.78
(*S*)-(−)-**CDX-2**	−5.2		First	
(*R*)-(−)-**CDX-3**	−4.9	0.9	First	5.02
(*S*)-(+)-**CDX-3**	−5.8		Second	
(*R*)-(+)-**CDX-4**	−4.7	0.0	–	1.00
(*S*)-(−)-**CDX-4**	−4.7		–	
(*R*)-(−)-**CDX-5**	−4.6	−0.1[2]	–	1.00
(*S*)-(+)-**CDX-5**	−4.5		–	
(*R*)-(+)-**CDX-6**	−4.6	−0.1[2]	–	1.00
(*S*)-(−)-**CDX-6**	−4.5		–	
(*R*)-(−)-**CDX-7**	−4.6	−0.1[2]	–	1.00
(*S*)-(+)-**CDX-7**	−4.7		–	

CDX, chiral derivative of xanthone.
[1]MeOH inside the selector cleft.
[2]Energy differences not considered significant.

Compared to the enantioseparated CDXs (**1–3**), an alkyl group bonded to the stereogenic center exists on **CDX-7** instead of the phenyl ring. Thus, the simultaneous π–π interactions that may be established by the phenyl ring at the stereogenic center as well as the xanthonic scaffold with the selector, as observed for CDXs **1–3**, are crucial for enantioresolution.

Bearing in mind the importance of H bonding and π–π interactions for the mechanism of chiral recognition for *(S,S)*-Whelk-O1, additional research was done in order to evaluate the frequency of these interactions among the total calculated conformations (Table 4). Given that AutoDock Vina retrieved nine conformations for each enantiomer of CDXs **1–7**, in a total of 126 conformations, it was found that the most frequent H-bonding interaction was with the amide H of the selector, whereas the most frequent π–π interactions were with the phenanthryl group (Table 4).

The interactions established by the xanthonic scaffold of all enantiomeric pairs of CDXs (**1–7**) were also examined, with the carbonyl group participating in more H-bonding interactions than the oxygen of the heterocyclic ring. Also, the xanthonic scaffold established more frequently π–π interactions with phenanthryl group than with 3,5-dinitrophenyl group of the selector.

An additional aspect of this study was the analysis of the influence of the presence of solvent molecules on the ligand binding affinity and on the ligand binding orientation. Docking results described in the literature have already shown that when solvent molecules were explicitly included in the docking calculations as a part of the receptor[61] or when solvent molecules were added by a Monte Carlo-based solvated docking approach,[62,63] the docking results are more in accordance with the experimental data.

TABLE 6. Calculated binding energy values of the lowest binding affinity conformation for each enantiomer of CDXs 1–7 on flexible (*S*,*S*)-Whelk-O1

CDX	Binding affinity (kcal.mol^{-1})	Energy difference (kcal.mol^{-1})	Elution order	α
(*R*)-(+)-**CDX-1**	−5.5	−0.3	Second	1.91
(*S*)-(−)-**CDX-1**	−5.2		First	
(*R*)-(+)-**CDX-2**	−5.6	−0.8	Second	2.47
(*S*)-(−)-**CDX-2**	−4.8		First	
(*R*)-(−)-**CDX-3**	−5.2	0.2	First	4.08
(*S*)-(+)-**CDX-3**	−5.4		Second	
(*R*)-(+)-**CDX-4**	−5.1	0.0	–	1.10
(*S*)-(−)-**CDX-4**	−5.1		–	
(*R*)-(−)-**CDX-5**	−5.1	0.0	–	1.06
(*S*)-(+)-**CDX-5**	−5.1		–	
(*R*)-(+)-**CDX-6**	−5.2	0.0	–	1.00
(*S*)-(−)-**CDX-6**	−5.2		–	
(*R*)-(−)-**CDX-7**	−5.1	0.0	–	1.00
(*S*)-(+)-**CDX-7**	−5.1		–	

CDX, chiral derivative of xanthone.

To obtain a complete description of (*S*,*S*)-Whelk-O1-ligand interactions, the study of potential solvent-mediated interactions was made. For this purpose, MeOH was used as an example of the influence of solvent molecules in the docking poses and scores of enantiomeric pairs of CDXs **1–7** (Table 5).

The docking calculations lead to a 100% successful reproduction of the enantioselectivity and elution order. Thus, it is shown that the accurate placement of explicit solvent into the systems can potentially improve docking results.

A final study revealed that the introduction of flexibility in the selector amide chain did not improve the overall docking scores results (Table 6).

CONCLUSION

The (*S*,*S*)-Whelk-O1 CSP showed the highest enantioselectivity and resolution for the enantiomeric pairs of CDXs evaluated, whereas the L-phenylglycine CSP showed the lowest discrimination ability. Actually, under the systematic chromatographic conditions evaluated, three out of seven enantiomeric pairs of CDXs (**1–3**) were enantioseparated on (*S*,*S*)-Whelk-O1 CSP, with α ranging from 1.91 to 7.55 and R_S ranging from 6.71 to 24.16. The highest resolutions were achieved for CDXs possessing an aromatic moiety bonded to the stereogenic center. Polar-organic conditions presented the best chromatographic parameters allowing good resolutions and lower run time than normal phase and reversed-phase conditions. The docking studies considering the results for (*S*, *S*)-Whelk-O1 CSP yielded scores that were in accordance with the chromatographic results regarding enantioselectivity and the enantiomer elution order. The selector solvation and the flexibility of the amide chain were also considered on docking calculations. The simultaneous π–π interactions that may be established by the substituent phenyl group at the stereogenic center as well as the xanthonic scaffold with the selector demonstrated to be essential for enantioselective recognition.

The results of the present study fulfilled the initial objectives regarding separation of CDXs and further elucidation of the intermolecular CSP–CDXs interactions.

LITERATURE CITED

1. Zhang Y, Wu DR, Wang-Iverson DB, Tymiak AA. Enantioselective chromatography in drug discovery. Drug Discov Today 2005;10(8):571–577.
2. Ward TJ, Ward KD. Chiral separations: fundamental review 2010. Anal Chem 2010;82:4712–4722.
3. Cavazzini A, Pasti L, Massi A, Marchetti N, Dondi F. Recent applications in chiral high performance liquid chromatography: a review. Anal Chim Acta 2011;706:205–222.
4. Welch CJ. Evolution of chiral stationary phase design in the Pirkle laboratories. J Chromatogr A 1994;666:3–26.
5. Lämmerhofer M. Chiral recognition by enantioselective liquid chromatography: mechanisms and modern chiral stationary phases. J Chromatogr A 2010;1217:814–856.
6. Pirkle WH, Däppen R. Reciprocity in chiral recognition. Comparison of several chiral stationary phases. J Chromatogr A 1987;404:107–115.
7. Pirkle WH, Hyun MH, Tsipouras A, Hamper BC, Banks B. A rational approach to the design of highly effective chiral stationary phases for the liquid chromatographic separation of enantiomers. J Pharm Biomed Anal 1984;2:173–181.
8. Pirkle WH, Hyun MH. Preparation and use of hydantoin-based chiral stationary phases. J Chromatogr A 1985;322:309–320.
9. Pirkle WH, Selness SR. Chiral recognition studies: intra- and intermolecular 1H{1H}-nuclear overhauser effects as effective tools in the study of bimolecular complexes. J Org Chem 1995;60:3252–3256.
10. Pirkle WH, Murray PG, Wilson SR. X-ray crystallographic evidence in support of a proposed chiral recognition mechanism. J Org Chem 1996;61:4775–4777.
11. Gasparrini F, Misiti D, Villani C. High-performance liquid chromatography chiral stationary phases based on low-molecular-mass selectors. J Chromatogr A 2001;906:35–50.
12. Yilmaz H, Topal G, Cakmak R, Hosgoren H. Resolution of (±)-β-methylphenylethylamine by a novel chiral stationary phase for Pirkle-type column chromatography. Chirality 2010;22:252–257.
13. Moiteiro C, Fonseca N, Curto MJM, Tavares R, Lobo AM, Ribeiro-Claro P, Félix V, Drew MGB. Development of novel brush-type chiral stationary phases based on terpenoid selectors: HPLC evaluation and theoretical investigation of enantioselective binding interactions. Tetrahedron-Asymmetry 2006;17:3248–3264.
14. Pinto M, Tiritan ME, Fernandes C, Cass Q. Fases Estacionárias Quirais baseadas em Derivados Xantónicos. Boletim da Propriedade Industrial nº 2011/01/21, Patent PT 104679 2011.
15. Pirkle WH, Welch CJ. An improved chiral stationary phase for the chromatographic separation of underivatized naproxen enantiomers. J Liq Chrom 1992;15:1947–1955.
16. Pirkle WH, Welch CJ. Use of simultaneous face to face and face to edge π–π interactions to facilitate chiral recognition. Tetrahedron-Asymmetry 1994;5:777–780.

17. Pirkle WH, Koscho ME, Wu Z. High-performance liquid chromatographic separation of the enantiomers of N-aryloxazolinones, N-aryl thiazolinones and their sulfur derivatives on a synthetic chiral stationary phase. J Chromatogr A 1996;726:91–97.
18. Pirkle WH, Brice LJ, Caccamese S, Principato G, Failla S. Facile separation of the enantiomers of diethyl N-(aryl)-1-amino-1-arylmethanephosphonates on a rationally designed chiral stationary phase. J Chromatogr A 1996;721:241–246.
19. Perera RWH, Lough WJ. Assessment of chiral stationary phases for suitability for combined enantiomeric impurity/related substances assays. J Chromatogr A 2011;1218:8655–8663.
20. Badaloni E, Cabri W, Ciogli A, D'Acquarica I, Deias R, Gasparrini F, Giorgi F, Kotoni D, Villani C. Extending the use of "Inverted Chirality Columns Approach" for enantiomeric excess determination in absence of reference samples: application to a water-soluble camptothecin derivative. J Chromatogr A 2010;1217:1024–1032.
21. Pirkle WH, Gan KZ. Facile and predictable means of separating the enantiomers of 5- arylhydantoins. J Chromatogr A 1997;790: 65–71.
22. Welch CJ, Szczerba T, Perrin SR. Some recent high-performance liquid chromatography separations of the enantiomers of pharmaceuticals and other compounds using the Whelk-O 1 chiral stationary phase. J Chromatogr A 1997;758:93–98.
23. Pirkle WH, House DW, Finn JM. Broad spectrum resolution of optical isomers using chiral high-performance liquid chromatographic bonded phases. J Chromatogr 1980;192:143–158.
24. Pirkle WH, Murray PG. The separation of the enantiomers of a variety of non-steroidal anti-inflammatory drugs (NSAIDS) as their anilide derivatives using a chiral stationary phase. J Liq Chrom 1990;13:2123–2134.
25. Pirkle WH, Tsipouras A. Direct liquid chromatographic separation of benzodiazepinone enantiomers. J Chromatogr 1984;291:291–298.
26. Lipkowitz KB. Atomistic modeling of enantioselection in chromatography. J Chromatogr A 2001;906:417–442.
27. Del Rio A, Hayes JM, Stein M, Piras P, Roussel C. Theoretical reassessment of Whelk-O1 as an enantioselective receptor for 1-(4-halogeno-phenyl)-1-ethylamine derivatives. Chirality 2004;16: S1-S11.
28. Del Rio A, Piras P, Roussel C. Enantiophore modeling in 3D-QSAR. A data mining application on Whelk-O1 chiral stationary phase. Chirality 2006;18: 498–508.
29. Del Rio A, Piras P, Roussel C. Data mining and enantiophore studies on chiral stationary phases used in HPLC separation. Chirality 2005;17: S74-S83.
30. Zhao C, Cann NM. Solvation of the Whelk-O1 chiral stationary phase: a molecular dynamics study. J Chromatogr A 2006;1131:110–129.
31. Zhao C, Cann NM. The docking of chiral epoxides on the Whelk-O1 stationary phase: a molecular dynamics study. J Chromatogr A 2007;1149:197–218.
32. Zhao CF, Diemert S, Cann NM. Rational optimization of the Whelk-O1 chiral stationary phase using molecular dynamics simulations. J Chromatogr A 2009;1216:5968–5978.
33. Pinto MMM, Sousa ME, Nascimento MSJ. Xanthone derivatives: new insights in biological activities. Curr Med Chem 2005;12: 2517–2538.
34. Correia-Da-Silva M, Sousa E, Duarte B, Marques F, Carvalho F, Cunha-Ribeiro LM, Pinto MMM. Polysulfated xanthones: multipathway development of a new generation of dual anticoagulant/ antiplatelet agents. J Med Chem 2011;54:5373–5384.
35. Paiva AM, Sousa ME, Camões A, Nascimento MSJ, Pinto MMM. Prenylated xanthones: antiproliferative effects and enhancement of the growth inhibitory action of 4-hydroxytamoxifen in estrogen receptor-positive breast cancer cell line. Medl Chem Res 2011:1–7.
36. Palmeira A, Vasconcelos MH, Paiva A, Fernandes MX, Pinto M, Sousa E. Dual inhibitors of P-glycoprotein and tumor cell growth: (re)discovering thioxanthones. Biochem Pharmacol 2012;83:57–68.
37. Palmeira A, Paiva A, Sousa E, Seca H, Almeida GM, Lima RT, Fernandes MX, Pinto M, Vasconcelos MH. Insights into the in vitro antitumor mechanism of action of a new pyranoxanthone. Chem Biol Drug Des 2010;76:43–58.
38. Castanheiro RAP, Pinto MMM, Silva AMS, Cravo SMM, Gales L, Damas AM, Nazareth N, Nascimento MSJ, Eaton G. Dihydroxyxanthones prenylated derivatives: synthesis, structure elucidation, and growth inhibitory activity on human tumor cell lines with improvement of selectivity for MCF-7. Bioorg Med Chem 2007;15: 6080–6088.
39. Costa E, Sousa E, Nazareth N, Nascimento MSJ, Pinto MMM. Synthesis of xanthones and benzophenones as inhibitors of tumor cell growth. Lett Drug Des Discovery 2010;7:487–493.
40. Sousa EP, Silva AMS, Pinto MMM, Pedro MM, Cerqueira FAM, Nascimento MSJ. Isomeric kielcorins and dihydroxyxanthones: synthesis, structure elucidation, and inhibitory activities of growth of human cancer cell lines and on the proliferation of human lymphocytes in vitro. Helv Chim Acta 2002;85:2862–2876.
41. Marona H, Szkaradek N, Karczewska E, Trojanowska D, Budak A, Bober P, Przepiórka W, Cegla M, Szneler E. Antifungal and antibacterial activity of the newly synthesized 2-xanthone derivatives. Arch Pharm (Weinheim) 2009;342:9–18.
42. Marona H, Pekala E, Antkiewicz-Michaluk L, Walczak M, Szneler E. Anticonvulsant activity of some xanthone derivatives. Bioorg Med Chem 2008;16:7234–7244.
43. Marona H, Szkaradek N, Rapacz A, Filipek B, Dybała M, Siwek A, Cegła M, Szneler E. Preliminary evaluation of pharmacological properties of some xanthone derivatives. Bioorg Med Chem 2009;17: 1345–1352.
44. Jastrzebska-Wiesek M, Librowski T, Czarnecki R, Marona H, Nowak G. Central activity of new xanthone derivatives with chiral center in some pharmacological tests in mice. Pol J Pharmacol 2003;55: 461–465.
45. Jastrzbska-Wisek M, Czarnecki R, Marona H. The anticonvulsant, local anesthetic and hemodynamic properties of some chiral aminobutanol derivatives of xanthone. Acta Pol Pharm Drug Res 2008;65: 591–600.
46. Marona H, Librowski T, Cegła M, Erdoan C, ahin NÖ. Antiarrhythmic and antihypertensive activity of some xanthone derivatives. Acta Pol Pharm Drug Res 2008;65:383–390.
47. Fernandes C, Tiritan ME, Cass Q, Kairys V, Fernandes MX, Pinto M. Enantioseparation and chiral recognition mechanism of new chiral derivatives of xanthones on macrocyclic antibiotic stationary phases. J Chromatogr A 2012;1241:60–68.
48. Koscho ME, Pirkle WH. Investigation of a broadly applicable chiral selector used in enantioselective chromatography (Whelk-O 1) as a chiral solvating agent for NMR determination of enantiomeric composition. Tetrahedron-Asymmetry 2005;16:3345–3351.
49. Koscho ME, Spence PL, Pirkle WH. Chiral recognition in the solid state: crystallographically characterized diastereomeric co-crystals between a synthetic chiral selector (Whelk-O1) and a representative chiral analyte. Tetrahedron-Asymmetry 2005;16:3147–3153.
50. Froimowitz M. HyperChem: a software package for computational chemistry and molecular modeling. Biotechniques 1993;14: 1010–3.
51. Mikhailopulo IA, Sokolov YA, He J, Chittepu P, Rosemeyer H, Seela F. Comparative conformational analysis of nucleosides by NMR, X-ray, and semi-empirical (PM3 VS. AM1) methods. Nucleos Nucleot Nucl 2005;24: 701–5.
52. Trott O, Olson AJ. AutoDock Vina: improving the speed and accuracy of docking with a new scoring function, efficient optimization, and multithreading. J Comput Chem 2010;31:455–61.
53. Lill MA, Danielson ML. Computer-aided drug design platform using PyMOL. J Comput Aided Mol Des 2010;25:13–9.
54. Dungelov J, Lehotay J, Cizmarik J, Armstrong D. Study of the mechanism of enantioseparation. IV. Study of enantioseparation of some derivatives of phenylcarbamic acid using π-complex stationary phase in HPLC. J Liq Chrom Rel Technol 2003;26:2331–2350.
55. Zheng J, Shamsi SA. Brush-type chiral stationary phase for enantioseparation of acidic compounds: optimization of chiral capillary electrochromatographic parameters. J Chromatogr A 2003;1005:177–187.
56. Asnin L, Gritti F, Kaczmarski K, Guiochon G. Features of the adsorption of naproxen on the chiral stationary phase (S,S)-Whelk-O1 under reversed-phase conditions. J Chromatogr A 2010;1217:264–275.
57. Asnin LD, Guiochon G. Retention of Naproxen enantiomers on the chiral stationary phase Whelk-O1 under reversed-phase conditions. A reconsideration of the adsorption mechanism in the light of new experimental data. J Chromatogr A 2010;1217:1709–1711.

58. Asnin LD, Guiochon G. The adsorption of naproxen enantiomers on the chiral stationary phase (R, R)-Whelk-O1 under reversed-phase conditions: the effect of mobile phase composition. J Chromatogr A 2010;1217: 2871–2878.

59. Asnin L, Kaczmarski K, Guiochon G. The adsorption of naproxen enantiomers on the chiral stationary phase Whelk-O1 under reversed-phase conditions: the effect of buffer composition. J Chromatogr A 2010;1217:7055–7064.

60. Seeliger D, de Groot BL. Ligand docking and binding site analysis with PyMOL and Autodock/Vina. J Comput Aided Mol Des 2010;24:417–22.

61. Frembgen-Kesner T, Elcock AH. Computational sampling of a cryptic drug binding site in a protein receptor: explicit solvent molecular dynamics and inhibitor docking to p38 MAP kinase. J Mol Biol 2006;359: 202–14.

62. Hixson CA, Benigni JP, Earl DJ. Solvent-shift Monte Carlo: a cluster algorithm for solvated systems. Phys Chem Chem Phys 2009;11: 6335–8.

63. Adamczyk P, Polanowski P, Sikorski A. Percolation in polymer-solvent systems: a Monte Carlo study. J Chem Phys 2009;131: 234901.